The complex non resonant double Hopf degeneracy: An alternative approach

Griselda R. Itovich
Dept. of Mathematics, FaEA
Universidad Nacional del Comahue
Buenos Aires 1400, (8300) Neuquén, Argentina
Email: gitovich@arnet.com.ar

Jorge L. Moiola
Dept. of Electrical Engineering and Computers
Universidad Nacional del Sur and CONICET
Av. Alem 1253, (8000) Bahía Blanca, Argentina
Email: jmoiola@criba.edu.ar

***Abstract*— The analysis of the complex non resonant double Hopf bifurcation is carried out by two complementary techniques: the frequency domain methodology and the normal form theory. Neimark-Sacker branches, which are originated at the singularity, are built precisely, thanks to the evaluation of Floquet multipliers of the nearby limit cycles. The quasi-analytical expressions of these solutions are obtained through the graphical Hopf theorem and higher order harmonic balance, which guarantees the accuracy of the results. The outcomes have been contrasted with LOCBIF software.**

I. Introduction

Hopf degeneracies are singularities in which some of the classical postulates of the Hopf bifurcation theorem fail. These degeneracies can give place to dynamic scenarios of different complexity such as multiple Hopf points in the equilibrium manifold, multiple occurrence of limit cycles, or the combination of both. Golubitsky and Langford [1] studied them using the mathematical machinery of singularity theory. Moreover, the analysis of other singularities involving multiple crossing of eigenvalues on the imaginary axis requires the ability to use different techniques such as normal forms, multiples scales, harmonic balance, just to mention only a few. This article treats a particular degeneracy known as non resonant double Hopf (*DH*) bifurcation (also called Hopf-Hopf bifurcation) which happens when the linearization of the flow evaluated at one equilibrium point has two pairs of imaginary pure eigenvalues $\pm i\omega_1$, $\pm i\omega_2$ where the quotient ω_1/ω_2 is an irrational number and no other eigenvalues exist with zero real part [2]. In these terms, the analysis can be reduced always to a four dimensional problem. Several engineering models, specially those concerning coupled oscillators in mechanical systems, present this singularity [3,4]. In these articles, the authors have shown the birth of quasiperiodic motion (also called secondary Hopf bifurcation or Neimark-Sacker bifurcation) of different complexity besides the classical oscillatory behavior emanating from Hopf bifurcations.

Nowadays, the *DH* degeneracy can be analyzed by normal form theory through a computation of symbolic algebraic systems [5]. Furthermore, it is shown in [2] how to determine if the appearance of quasiperiodic solutions involves two modes (or 2D-tori, which is called the *simple* case), or if the quasiperiodicity involves three oscillatory modes (or 3D-tori, which is known as the *complex* case). Occasionally, this last phenomenon can be exhibited as the first pattern of a route to chaos in high-dimensional systems after generating a sequence of Neimark-Sacker bifurcations [6]. On the other hand, the graphical Hopf theorem [7] and its extensions [8,9] provide tools that can be complemented with Floquet theory to study the dynamics in the neighborhood of the emerging limit cycle. Then, local bifurcations of the limit cycles can be analyzed in the vicinity of the *DH* bifurcation condition [10]. This approach would be valuable specially when one has interest in studying bifurcation or cyclic bifurcation control [11,12]. Hence, the precise determination of the Hopf bifurcation curve together with both Neimark-Sacker bifurcation branches originated at *DH*, enables us to recognize certain regions in the parameter space close to the singularity. The involved dynamics is distinctive [13] and confirms the classical results [2]. Taking into account the frequency domain setting along with the outcomes obtained through normal form theory, the complex case has been analyzed. Thus, regions where the 3D-tori appear have been located and their existence has been checked through numerical simulations. Moreover, cyclic fold and period-doubling bifurcations, 1-codimension Hopf degeneracies and some resonances have been found close to the singularity. These determinations allow to deepen and complete the analysis of the intrincate dynamic scenario around *DH*.

II. The frequency domain approach for Hopf bifurcation

The analysis is focused on the autonomous nonlinear system

$$\dot{x} = f(x;\eta), \tag{1}$$

where $x \in R^n$, $\dot{x} = \frac{dx}{dt}$, $\eta \in R^m$ is a bifurcation parameter vector and $f \in C^9$ in its first variable. Some particular dynamic changes in the solutions of (1) are detected through bifurcation points. For instance, if $\eta \in R^1$ one can study the Hopf bifurcation (HB) phenomenon which is related with the appearance of periodic solutions under the variation of η whereas an equilibrium point changes its stability (a stable focus changes to unstable one, or vice versa). In the time domain setting, this situation is found through the eigenvalues

of the Jacobian matrix $\frac{\partial f}{\partial x}$, evaluated at the steady state: A necessary condition for HB is a single pair of complex eigenvalues crossing the imaginary axis. This paper is based on an alternative approach, which comes through feedback systems and control theory. The bifurcations are found in the frequency domain, by using the Laplace transform and the method of harmonic balance. The system (1) is now written as

$$\begin{aligned} \dot{x} = &\quad A(\eta)x + B(\eta)\left[D(\eta)y + u\right], \quad y = C(\eta)x, \\ u = &\quad g(e;\eta) = \tilde{g}(y;\eta) - D(\eta)y, \end{aligned} \tag{2}$$

where $y \in R^l$ is the output variable and, $u \in R^p$ is a nonlinear control variable which acts as an input for the new system. The $n \times n$ matrix A is considered invertible for every value of η while B, C and D are $n \times p$, $l \times n$ and $p \times l$ matrices, respectively; besides $\tilde{g} \in R^p$ is a smooth nonlinear function which results from the initial function f in (1) and the selected matrices. It is supposed that $e = -y$. Applying Laplace transform to (2) with the initial condition $x(0) = 0$, yields

$$e = -G(0;\eta)g(e;\eta), \tag{3}$$

where $G(s;\eta) = C[sI-(A+BDC)]^{-1}B$ is the usual transfer matrix of the linear part of system (2). Now, the solutions of the equation (3) are considered as the steady states of (2) in the frequency domain. Suppose that $\tilde{x}$ and $\tilde{e}$ be the equilibrium points of the equation (1) and its corresponding counterpart in the frequency domain, respectively. In these terms, the bifurcation analysis results from the $l \times l$ matrix $G(s;\eta)J(\eta)$, where

$$J(\eta) = D_1 g(e;\eta)|_{e=\tilde{e}} = \left[\left.\frac{\partial g_j}{\partial e_k}\right|_{e=\tilde{e}}\right],$$

$g = [g_j]_{j=1}^{p}$, $e = [e_k]_{k=1}^{l}$. If there is a bifurcation in the solutions of system (2) for $\eta = \eta_0$ then, due to the generalized Nyquist stability criterion, one eigenvalue of the matrix $G(s;\eta)J(\eta)$ crosses $(-1+i0)$ when $s = i\omega_0$ and $\eta = \eta_0$. If the case deals with a Hopf or dynamic bifurcation one has $\omega_0 \neq 0$, which represents the starting frequency of the emergent periodic solution. Hence, considering the characteristic polynomial of the matrix GJ one defines

$$h(-1, i\omega_0; \eta_0) = \det(-1 * I - G(i\omega_0;\eta_0)J(\eta_0)) = 0,$$

which can be expressed as the following system

$$\begin{aligned} F_1(\omega_0, \eta_0) &= \mathrm{Re}[h(-1, i\omega_0; \eta_0)] = 0, \\ F_2(\omega_0, \eta_0) &= \mathrm{Im}[h(-1, i\omega_0; \eta_0)] = 0. \end{aligned} \tag{4}$$

This system yields a necessary condition to the existence of a bifurcation point (ω_0, η_0) in the frequency domain. Now, it is possible to establish the graphical Hopf theorem, *i.e.*, the version of the well known Hopf bifurcation theorem in the frequency domain:

Theorem 1:

H1) A unique solution $\hat{\lambda}$ (eigenvalue of the matrix GJ) of the equation $h(\lambda, i\omega; \eta) = 0$, crosses $(-1+i0)$ for a certain value $\omega = \omega_0 \neq 0$ (unique too) when $\eta = \eta_0$ and the equilibrium $\tilde{e}$ exhibits a stability change. Moreover, $\frac{\partial F_1}{\partial \omega}\big|_{(\omega_0,\eta_0)}$, $\frac{\partial F_2}{\partial \omega}\big|_{(\omega_0,\eta_0)}$ do not vanish simultaneously, where F_1 and F_2 have been defined in (4),

H2) The determinant

$$M_1 = \left|\left.\frac{\partial(F_1, F_2)}{\partial(\omega, \eta)}\right|_{(\omega_0,\eta_0)}\right| = \left|\begin{array}{cc} \frac{\partial F_1}{\partial \omega} & \frac{\partial F_1}{\partial \eta} \\ \frac{\partial F_2}{\partial \omega} & \frac{\partial F_2}{\partial \eta} \end{array}\right|_{(\omega_0,\eta_0)},$$

is nonzero,

H3) The curvature coefficient (also known as the first Lyapunov coefficient) defined as

$$\sigma_1 = -\,\mathrm{Re}\left(\frac{w^T G(i\omega_0;\eta_0)p_1(\omega_0,\eta_0)}{w^T G'(i\omega_0;\eta_0)J(\eta_0)v}\right), \tag{5}$$

has sign definition.

Then the system (1) has one branch of periodic solutions which starts at $\eta = \eta_0$, and its direction and stability depend on the signs of M_1 and σ_1.

Proof: See [7,8].

Observation: In the expression (5), w^T and v are the normalized left and right eigenvectors of the matrix $G(i\omega_0;\eta_0)J(\eta_0)$ associated with the eigenvalue $\hat{\lambda}$ ($\bar{w}^T v = 1$ and $\bar{v}^T v = 1$, where " $\bar{\cdot}$ " means complex conjugation), $G' = \frac{dG}{ds}$ and p_1 is a $p-$dimensional vector with complex components

$$p_1(\omega,\eta) = QV_{02} + \frac{1}{2}\overline{Q}V_{22} + \frac{1}{8}L\overline{v}, \tag{6}$$

where the matrices Q, $\overline{Q}$ and L of order $p \times l$ are defined through the second and third derivatives of the function g [7]. Furthermore, the vectors in (6) are defined as

$$V_{02} = -\frac{1}{4}H(0;\eta)Q\overline{v},\ V_{11} = v,\ V_{22} = -\frac{1}{4}H(i2\omega;\eta)Qv, \tag{7}$$

where $H(s;\eta) = [I + G(s;\eta).J(\eta)]^{-1}\,G(s;\eta)$ is the closed-loop transfer matrix for the feedback system which comes with (2).

The demonstration is constructive and considers the intersection between two eigenlocus. One eigenlocus represents the Nyquist diagram of the linear part of the system while the other takes into account the nonlinear nature of the feedback. This last one is referred to as the amplitude locus. If an intersection exists for $\tilde{\eta}$ close to η_0, on the Nyquist type eigenlocus one reads the frequency $\hat{\omega}$ while on the amplitude locus one encounters an estimation of the size of the oscillation $\hat{\theta}$. Then it can be established an approximate formula for the orbit, employing a second order harmonic balance, as follows

$$e = e(t;\tilde{\eta}) = \tilde{e}(\tilde{\eta}) + \mathrm{Re}\left(\sum_{k=0}^{2} E_k^2 \exp(ik\hat{\omega}t)\right),$$

where

$$E_0^2 = \quad V_{02}\hat{\theta}^2, \quad E_1^2 = V_{11}\hat{\theta} + V_{13}\hat{\theta}^3, \quad E_2^2 = V_{22}\hat{\theta}^2,$$

according with (7) and the vector V_{13} can be computed as described in [8]. Considering higher order harmonic balance,

more precise expressions (but still of local validity) for the periodic solutions can be obtained [8]. A similar procedure (but up to eight harmonics) is implemented here to compute limit cycle approximations using the so-called modified scheme (noted as MS) in [9] when the original one proposed in [7] and [8] does not reach a suitable intersection between both loci.

III. Stability of cycles and its local bifurcations

The stability of one $T-$periodic solution $X = X(t;\tilde{\eta})$ of the equation (1) can be evaluated through the eigenvalues of its monodromy matrix, also called Floquet multipliers. The $n \times n$ monodromy matrix is $M(T)$ where $M = M(t)$ solves the differential matrix equation:

$$\dot{M} = S(t)M,$$

where $\dot{M} = \frac{dM}{dt}$, and $S(t) = D_1 f(X(t;\tilde{\eta});\tilde{\eta}) = \left.\frac{\partial f}{\partial x}\right|_{x=X(t;\tilde{\eta}),\eta=\tilde{\eta}}$, $S(t+T) = S(t)$, where T is the period of the orbit X. It is established as the initial condition $M(0) = I$, where I is the identity matrix of order n. The $n-$eigenvalues of $M(T)$ are $\beta_0 = 1$, the trivial multiplier due to the analysis of the flow on a cycle, and the remaining $\beta_i,\ i = 1, 2, \cdots, n-1$. If $|\beta_i| < 1$ for each i then X results stable. On the contrary if $|\beta_j| > 1$, for some j, then the orbit X is unstable. The crossing of the unit circle by at least one β_j defines one local cyclic bifurcation. If β_j crosses the frontier through the positive real axis, *i.e.*, $\beta_j = 1$, then a fold, transcritical or pitchfork bifurcation is detected. On the other hand, if $\beta_j = -1$ a period-doubling bifurcation is established. The simultaneous crossing of a complex conjugate pair of Floquet multipliers defines a Neimark-Sacker or secondary Hopf bifurcation. The latter is related with the appearance of quasiperiodic solutions, which almost cover some torus surfaces in the state space. The Hopf singularity that will be considered is fully connected with this last type of cyclic bifurcation.

IV. Double Hopf bifurcation

From now on, a particular Hopf degeneracy, due to the failure of **H1** of Theorem 1 in Section II is considered: the non resonant double Hopf bifurcation, which appears when the linearization of the system (1) about one equilibrium point, for some parameter value η_0, has two pairs of eigenvalues $\pm i\omega_1, \pm i\omega_2,\ \omega_1/\omega_2 \in I$, where $\omega_1 > \omega_2 > 0$. The dynamic scenario can be described completely in the four dimensional center manifold with two independent bifurcation parameters, say $\eta = (\eta_1, \eta_2)$. However, normal form theory and the frequency domain method give alternative procedures to deepen the analysis of the singularity.

A. Using normal form theory

It is sufficient to consider the system

$$\dot{x} = f(x;\eta), \tag{8}$$

where $x \in R^4,\ \eta = (\eta_1, \eta_2) \in R^2$. Suppose that one has a *DH* at the equilibrium $x = 0$ and $\eta = 0$, with frequencies ω_1 and ω_2, as described above. Employing the method of multiple scales, a normal form with terms up to third order is achieved [5], which can be expressed in polar coordinates in the following way

$$\begin{array}{ll} \dot{r}_1 = & r_1(\alpha_{11}\eta_1 + \alpha_{12}\eta_2 + p_{11}r_1^2 + p_{12}r_2^2), \\ \dot{r}_2 = & r_2(\alpha_{21}\eta_1 + \alpha_{22}\eta_2 + p_{21}r_1^2 + p_{22}r_2^2), \\ \dot{\varphi}_1 = & \omega_1 + \psi_1(r_1, r_2; \eta), \\ \dot{\varphi}_2 = & \omega_2 + \psi_2(r_1, r_2; \eta), \end{array} \tag{9}$$

where $\psi_i(r_1, r_2; \eta) = \xi_{i1}\eta_1 + \xi_{i2}\eta_2 + q_{i1}r_1^2 + q_{i2}r_2^2,\ i = 1, 2$ and $\alpha_{ij},\ p_{ij},\ \xi_{ij},\ q_{ij},\ i, j = 1, 2$, are constants. The equilibrium points can be easily found now, solving $\dot{r}_1 = \dot{r}_2 = 0$, in the two dimensional system. Thus, if $r_1 \neq 0$ and $r_2 \neq 0$, one obtains

$$E : r_1^2 = (p_{12}\Omega_2 - p_{22}\Omega_1)\,\Delta^{-1},\ r_2^2 = (p_{21}\Omega_1 - p_{11}\Omega_2)\,\Delta^{-1},$$

where $\Omega_1 = \alpha_{11}\eta_1 + \alpha_{12}\eta_2,\ \ \Omega_2 = \alpha_{21}\eta_1 + \alpha_{22}\eta_2$, $\Delta = p_{11}p_{22} - p_{12}p_{21} \neq 0$, which represents a quasiperiodic solution or 2D-torus with approximate frequencies $\tilde{\omega}_1$ and $\tilde{\omega}_2$, close to ω_1 and ω_2, respectively, in the fourth-order system.

The analysis is based on the cases with $p_{11}p_{22} > 0$ or $p_{11}p_{22} < 0$. Particularly, the case where $p_{11}p_{22} > 0$ is considered as the *simple* one due to the planar system determined through the first two equations of (9) does not show periodic solutions. The appearance of periodic solutions would correspond to Hopf bifurcations of the equilibrium points E noted above, originating the so-called 3D-torus in the fourth-order system.

In the $\eta-$plane the Hopf bifurcation curve can be plotted as well as two branches of Neimark-Sacker or torus bifurcation curves, T_1 and T_2, where the above-mentioned 2D-tori arise. Otherwise, when the *complex* case is treated, say $p_{11}p_{22} < 0$, and considering $p_{11} > 0,\ p_{22} < 0$, the analysis is established on the variables $\rho = p_{12}p_{22}^{-1},\ \delta = p_{21}p_{11}^{-1}$ (it is known that $\rho\delta - 1 \neq 0$). Particularly, solutions coming from the Hopf bifurcations of quasiperiodic solutions, called 3D-tori, can appear with $\rho \geq \delta, \rho < 0$ and $\rho\delta > 1$. An schematic representation of the bifurcation curves in the neighborhood of the *DH* singularity associated to this configuration is shown in Figure 1. The axes τ_1, τ_2 are the tangent lines of Hopf bifurcation curves in the fourth-order system at $\eta = 0$. The curve C is the bifurcation curve of the equilibriums of type E. Moreover, Y is the curve where the new periodic solutions disappear, in a heteroclinic bifurcation. Taking into account the partition of the neighborhood of the origin in the $\tau-$plane, as can be observed in Figure 1, one finds that in regions 1 and 3 appear an equilibrium and one limit cycle which is unstable, while zone 2 only shows an unstable equilibrium. Regions 4 to 8 exhibit one unstable equilibrium and two cycles. Particularly, the dynamics of regions 5, 6 and 7 includes a 2D-tori while a 3D-torus only appears between C and Y (called region 6). Specifically, Yu [5] gives a methodology, starting from the truncated normal form (9), to determine the tangent lines to the

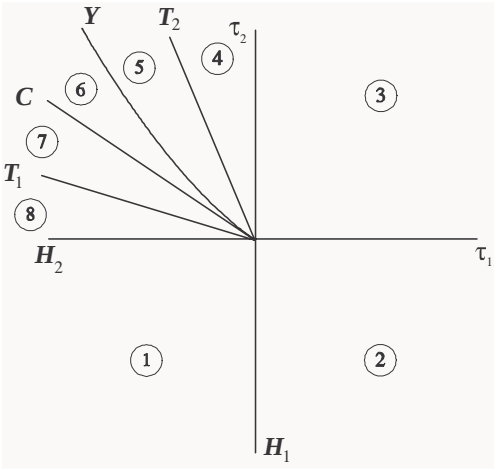

Fig. 1. Schematic representation of the bifurcation curves close to the singularity *DH* with $\delta \leq \rho$, $\rho < 0$ and $\rho\delta > 1$ (H_i, $i = 1, 2$ represent the tangent lines to the Hopf bifurcation branches at criticality while T_i, $i = 1, 2$ are those to the Neimark-Sacker continuations). The numbers obey to a particular dynamic configuration in each of the eight regions [2].

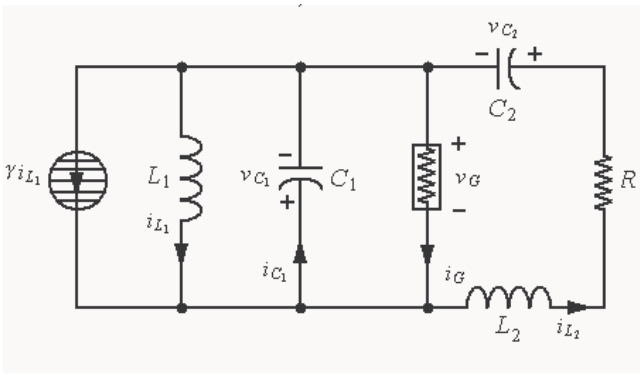

Fig. 2. A doubly LCR coupled electrical circuit ($\gamma = \eta_3\eta_1^{-1}$).

Neimark-Sacker bifurcation curves, T_1 and T_2, whose origin is the non resonant double Hopf point, and also to the curve C, where the 3D-torus solution emerges.

B. Under a frequency domain methodology

Once a *DH* point is detected, again for simplicity, suppose at the equilibrium $x = 0$ with $\eta = 0$, the Hopf bifurcation curve that traverses the singularity in the $\eta-$plane can be built just considering the system (4) with the starting points $(\omega_i, 0)$, $i = 1, 2$. This reveals a curled curve and one distinctive autointersection point: the *DH* singularity. Each branch is associated with one of the frequencies and it is possible to get high accurate quasianalytical approximations of the emerging cycles, employing the generalizations of Theorem 1 (the graphical Hopf theorem). The analysis of the evolution of its Floquet multipliers of the periodic solutions, following the ideas in Section III, allows to detect cyclic bifurcations. Particularly, two Neimark-Sacker branches emerge from the singularity, generating a tricky dynamic region in the $\eta-$plane, which includes the existence of 3D-tori.

V. Example

The considered nonlinear system is designed with two coupled LCR circuits as shown in Figure 2, where C_1, C_2 are capacitors and, L_1, L_2 are inductances and R is a resistor. Choosing the voltages across the capacitors and the currents in the inductances as state variables, one obtains

$$\begin{aligned}
\dot{x}_1 &= \eta_1(\tfrac{1}{2}x_1 - \alpha_2 x_1^2 - \alpha_3 x_1^3) + (\eta_1 + \eta_3)\, x_2 - \eta_1 x_4,\\
\dot{x}_2 &= -\tfrac{1}{2}\sqrt{2}\, x_1,\\
\dot{x}_3 &= (\sqrt{2}+1)x_4,\\
\dot{x}_4 &= (2-\sqrt{2})(x_1 - x_3 - \eta_2 x_4),
\end{aligned} \tag{10}$$

where $x = (x_1, x_2, x_3, x_4) = (v_{C_1}, i_{L_1}, v_{C_2}, i_{L_2})$, $\eta_1 = \frac{1}{C_1}$ and $\eta_2 = R$ are independent bifurcation parameters. The constants C_2, L_1 and L_2 have the following values: $C_2 = \frac{1}{\sqrt{2}+1}$, $L_1 = \frac{2}{\sqrt{2}}$ and $L_2 = \frac{1}{2-\sqrt{2}}$. In this case, the conductance is a nonlinear element which can be described according to the current-voltage nonlinear function $i_G = -\frac{1}{2}v_G - \alpha_2 v_G^2 + \alpha_3 v_G^3$, where two additional parameters, α_2 and α_3, are now included. Besides, the term $u = \eta_3 x_2$ in the first equation of system (10) appears due to a control function which depends on the second variable and a new auxiliary parameter. This model has been analyzed in detail for the case $(\alpha_2, \alpha_3) = (0, 1)$ and $\eta_3 = 0$ in [10].

It is easy to see that the unique equilibrium point of system (10) is $\tilde{x} = 0$, while $\eta_1 + \eta_3 \neq 0$. Considering the linearization of the system evaluated at the equilibrium, one finds a unique 1:1 resonant double Hopf singularity for $\eta^{**} = (\eta_1^{**}, \eta_2^{**}, \eta_3^{**}) = (4(2-\sqrt{2}), 2, 2(2\sqrt{2}-3))$ with frequency $\omega^{**} = \sqrt[4]{2}$. Moreover, one discovers close to this degeneracy infinite non resonant double Hopf points, which exist for $2(2\sqrt{2}-3) < \eta_3 < 2$. In this range of values, the case $\eta_3 = -0.22$ with the analysis of the dynamics close to a complex non resonant double Hopf singularity (in the sense of Section IV) will be the focus of the rest of this article.

Applying the methodology described in Section II, the system (10) is written as (2) defining

$$A = \begin{bmatrix} 0 & \eta_1+\eta_3 & 0 & -\eta_1 \\ -\frac{1}{2}\sqrt{2} & 0 & 0 & 0 \\ 0 & 0 & 0 & \sqrt{2}+1 \\ 2-\sqrt{2} & 0 & -(2-\sqrt{2}) & -(2-\sqrt{2})\eta_2 \end{bmatrix},$$

$$B = \begin{bmatrix} 1 & 0 & 0 & 0 \end{bmatrix}^T = C^T, \quad D = [\ 0\ ],$$

and $u = g(e; \eta_1, (\alpha_2, \alpha_3)) = \eta_1\left(-\frac{1}{2}e - \alpha_2 e^2 + \alpha_3 e^3\right)$, with $e = -y$. Then, it is possible to compute the transfer matrix G and to find the corresponding equilibrium equation (3) in the frequency domain, whose unique solution results $\tilde{e} = 0$. Thus, the characteristic and unique eigenvalue $\hat{\lambda}$ of GJ evaluated at $s = i\omega$, can be expressed as

$$\hat{\lambda} = (A_1 + iA_2)\,(A_3 + iA_4)^{-1}, \tag{11}$$

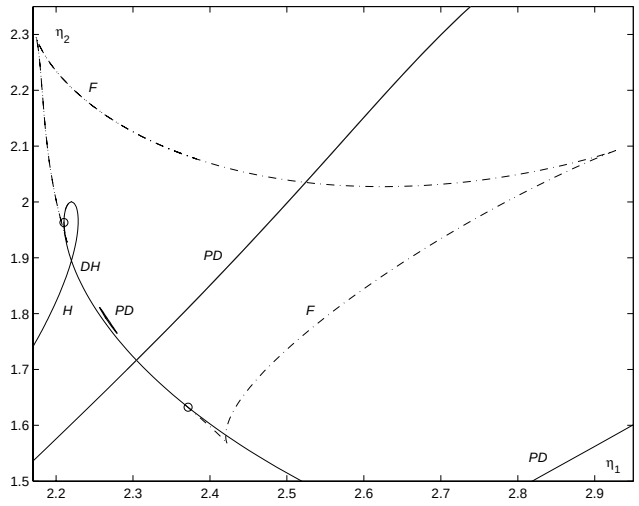

Fig. 3. Hopf bifurcation (H) curve through *DH* for $(\alpha_2, \alpha_3) = (0.6, 1)$ and $\eta_3 = -0.22$. (Cyclic fold (F) ($-.$) and period doubling bifurcation (PD) ($-$) curves in the neighborhood of *DH*, H_{10} Hopf degeneracies (o)).

where

$$A_1 = -\eta_1\eta_2\omega^2(2-\sqrt{2}), \quad A_2 = \eta_1\omega(\sqrt{2}-\omega^2),$$
$$A_3 = -2\omega^4 + (\kappa+\sqrt{2}\eta_3)\omega^2 - 2\chi,$$
$$A_4 = 2(2-\sqrt{2})\eta_2\omega^3 - 2(\sqrt{2}-1)\chi\eta_2\omega,$$

where $\kappa = \kappa(\eta_1) = (4-\sqrt{2})\eta_1 + 2\sqrt{2}$ and $\chi = \eta_1 + \eta_3$.

If $\eta_3 = -0.22$, it is found that the non resonant double Hopf singularity *DH* has coordinates $\eta_1 = 2.22$, $\eta_2 = 1.89488$ and its critical frequencies are $\bar{\omega}_1 = 1.065654287$, $\bar{\omega}_2 = 1.327084759$. With this starting point and solving the nonlinear system

$$F_1(\omega, \eta) = \mathrm{Re}(\hat{\lambda}) + 1 = 0, \qquad F_2(\omega, \eta) = \mathrm{Im}(\hat{\lambda}) = 0,$$

where the expression of $\hat{\lambda}$ is given by (11), a continuation of Hopf (H) bifurcation points can be done in the $\eta_1 - \eta_2$ parameter plane. Its two branches, named as $H_i,\ i = 1, 2$ are associated with the frequencies $\bar{\omega}_i,\ i = 1, 2$ respectively, and represented in Figure 3. Now, fixing $(\alpha_2, \alpha_3) = (0.6, 1)$ and for completeness, the fold (F) bifurcation curve and the period-doubling (PD) one, obtained with the LOCBIF software [14], have been added to the last figure. It must be observed the cyclic fold curve is similar to a curved triangle, incomplete in one of its sides. Its terminal or generating points are certain Hopf degeneracies $HD_i, i = 1, 2$, usually noted H_{10}, where the curvature coefficient σ_1 vanishes (see (5) in **H3** of Theorem 1), namely, $HD_1 : \eta_1 = 2.21033,\ \eta_2 = 1.96331,\ \omega = 1.1131983560,\ \sigma_1 = 0.646 * 10^{-7}$ and $HD_2 : \eta_1 = 2.37168,\ \eta_2 = 1.63223,\ \omega = 0.9837376553,\ \sigma_1 = -0.223 * 10^{-7}$. This kind of degeneracy is associated with the simultaneous coexistence of a pair of limit cycles in its unfolding. Moreover, the nearby period doubling curve is an island of period doubling bifurcations.

Keeping $\eta_3 = -0.22$ and fixing the value $\eta_2 = 1.88$, two Hopf bifurcation points are found close to *DH*, say, $\eta_1 = 2.21666$ for $\omega = 1.336433149$ (it belongs to H_2) and $\eta_1 = 2.22406$ for $\omega = 1.058200007$ (in H_1) (see Figure 4). Through the frequency domain methodology and considering quasianalytical expressions of higher order for the limit cycles, using the MS algorithm [9], and the evolution of their Floquet multipliers, two Neimark-Sacker bifurcation points are detected. The first one is obtained for $\eta_1 = 2.22816$, when a generic cycle, that appears from the H_2 branch, bifurcates. The second one results for $\eta_1 = 2.22476$, starting from the periodic solution born at H_1 branch. These detections are based on the results that are shown in Tables I and II, respectively. Repeating this procedure for a range of values $\eta_2 < 1.89488$ (the ordinate of the *DH* point), two Neimark-Sacker branches, which are born at *DH*, are built precisely and checked with the LOCBIF software as can be seen in Figure 4. The terminal points of these curves are another kind of degeneracies 1:2 resonance points (see [2] for more details) due to they belong to *PD* islands: the larger one has been mentioned before but there is also a tiny island situated above the right Hopf branch (see Figure 4).

TABLE I

DETECTION OF A NEIMARK-SACKER BIFURCATION OF CYCLES FOR η_2 = 1.88, WITH (α_2,α_3) = (0.6,1) AND η_3 = -0.22.

	$\eta_1 = 2.22816$	$\eta_1 = 2.22817$
β_0	1.001061337	1.001062903
β_{1-2}	$1.000011\exp(\pm 1.503911i)$	$0.999996\exp(\pm 1.504057i)$
β_3	0.9336322590	0.9335826414

TABLE II

DETECTION OF A SECOND NEIMARK-SACKER BIFURCATION OF CYCLES FOR η_2 = 1.88, WITH (α_2,α_3) = (0.6,1) AND η_3 = -0.22.

	$\eta_1 = 2.22476$	$\eta_1 = 2.22477$
β_0	1.005628287	1.005731349
β_{1-2}	$1.000144\exp(\pm 1.785426i)$	$0.999653\exp(\pm 1.787339i)$
β_3	0.9975715823	0.9975052464

Otherwise, by means of Yu's normal form implementation [5], one can obtain the tangent lines L_1, L_2 at *DH* to the Neimark-Sacker branches, proving the exactitude of the shown results, and get information about the existence of bifurcation of the arising 2D-tori. Specifically, it is possible to compute the tangent line L_3 to the curve C. If this line lays between L_1 and L_2 then a 3D-torus solution is possible. The expressions of these three lines are:

$$\begin{aligned} L_1: &\quad \eta_2 = -1.205744580(\eta_1 - 2.22) + 1.89488, \\ L_2: &\quad \eta_2 = -3.349711533(\eta_1 - 2.22) + 1.89488, \\ L_3: &\quad \eta_2 = -3.186850098(\eta_1 - 2.22) + 1.89488, \end{aligned}$$

and this is all shown in Figure 5. This situation agrees wholly with the dynamic portrait of Figure 1, and its adaptation to the analyzed configuration is given in Figure 6.

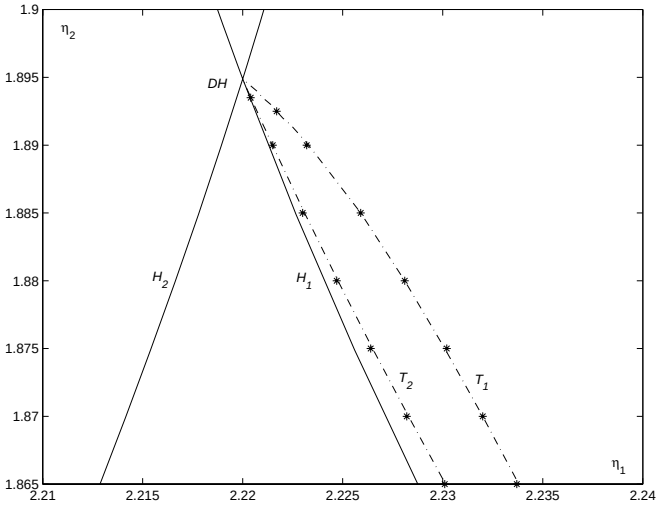

Fig. 4. Two Neimark-Sacker branches emanating from *DH* for $(\alpha_2, \alpha_3) = (0.6, 1)$ and $\eta_3 = -0.22$, obtained through the frequency domain methodology (FDM) $(-.)$. $((*)$ LOCBIF's results, $(-)$ Hopf bifurcation curve).

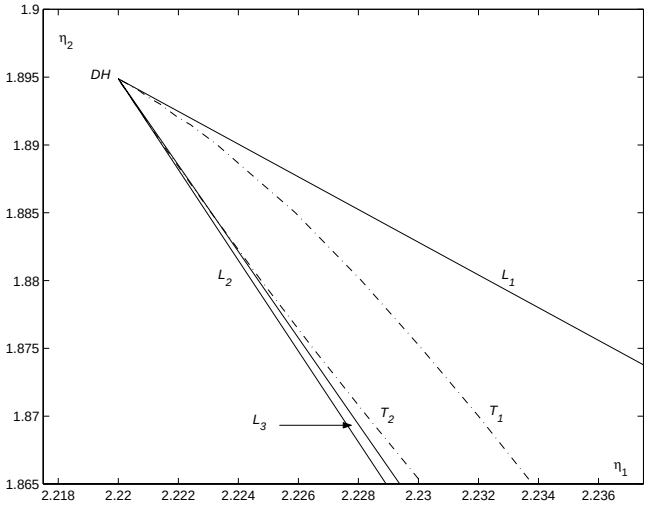

Fig. 5. The Neimark-Sacker T_1, T_2 $(-.)$ branches born at *DH*, through FDM, in conjunction with its tangent lines L_1, L_2 $(-)$ obtained by normal forms. L_3 $(-)$ is the tangent line to the curve C, where the 2D-torus bifurcates.

VI. Conclusions

The frequency domain methodology has allowed us to analyze partially the complex case of the non resonant double Hopf singularity. Specifically, particular dynamic regions in its neighborhood have been recognized thanks to the plotting of the Hopf bifurcation curve and the Neimark-Sacker branches. The normal form theory as well as LOCBIF have been used as complementary resources to check the appearance of the 2D and 3D-tori.

ACKNOWLEDGEMENT

The authors appreciate the financial support of UNCOMA (04E068), UNS (PGI 24K/30), ANPCyT (PICT 11-12524) and CONICET (PIP 5032).

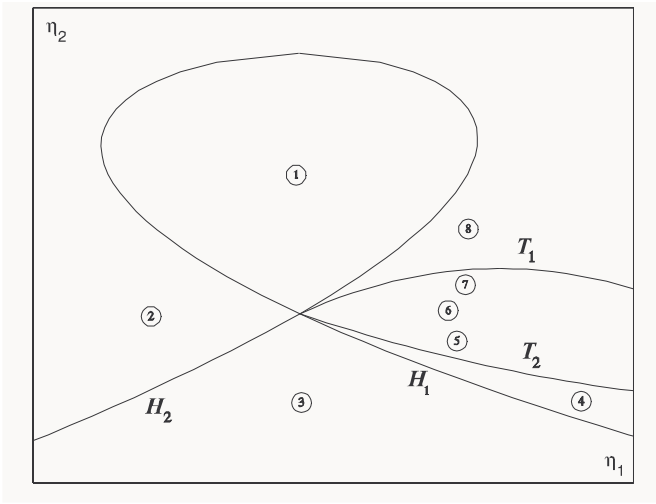

Fig. 6. Dynamics close to *DH* (complex case) for $(\alpha_2, \alpha_3) = (0.6, 1)$ and $\eta_3 = -0.22$. (H_i, $i = 1, 2$, are the Hopf branches, $T_i = NS_i$ $i = 1, 2$, are the Neimark-Sacker branches and the circled numbers are in correspondence with those of Figure 1).

References

[1] Golubitsky, M. and Langford, W. F. [1981]. "Classification and unfoldings of degenerate Hopf bifurcations," Journal of Differential Equations 41, 375-415.

[2] Kuznetsov, Y. A. [1998]. Elements of Applied Bifurcation Theory, Applied Mathematics Science 112, second edition. Springer-Verlag, New York.

[3] Gattulli, V., Di Fabio, F. and Luongo, A. [2001]. "Simple and double Hopf bifurcations in aeroelastic oscillators with tuned mass dampers," Journal of The Franklin Institute 338, 187-201.

[4] Chamara, P. A. and Coller, B. D. [2004]. "A study of double flutter," Journal of Fluids and Structures 19, 863-879.

[5] Yu, P. [2002]. "Analysis on double Hopf bifurcation using computer algebra with the aid of multiple scales," Nonlinear Dynamics 27, 19-53.

[6] Albers, D. J. and Sprott, J. C. [2006]. "Routes to chaos in high-dimensional dynamical systems: A qualitative numerical study," Physica D 223, 194-207.

[7] Mees, A. I. and Chua, L. [1979]. "The Hopf bifurcation theorem and its applications to nonlinear oscillations in circuits and systems," IEEE Transactions on Circuits and Systems 26 (4), 235-254.

[8] Mees, A. I. [1981]. Dynamics of Feedback Systems, John Wiley & Sons, Chichester, United Kingdom.

[9] Moiola, J. L. and Chen, G. [1996]. Hopf Bifurcation Analysis - A Frequency Domain Approach, Series A Vol. 21, World Scientific, Singapore.

[10] Itovich, G. R. and Moiola, J. L. [2005]. "Double Hopf bifurcation analysis using frequency domain approach," Nonlinear Dynamics 39, 235-258.

[11] Abed, E. H. and Fu, J. H. [1986]. "Local feedback stabilization and bifurcation control, I. Hopf bifurcation," Systems Control Letters 7, 11-17.

[12] Tesi, A., Abed, E. H., Genesio, R. and Wang, H. O. [1996]. "Harmonic balance analysis of period-doubling bifurcations with implications for control of nonlinear dynamics," Automatica 32, 1255-1271.

[13] Itovich, G. R. , Moiola, J. L. and Cendra, H. [2006]. "Complex dynamics close to a non resonant double Hopf bifurcation," 1st IFAC Conference on Analysis and Control of Chaotic Systems, CHAOS 2006, 255-260, Reims, France.

[14] Khibnik, A. I., Kuznetsov, Y. A., Levitin, V. V. and Nikolaev, E. V. [1993]. "Continuation techniques and interactive software for bifurcation analysis of ODE's and iterated maps," Physica D 62, 360-371.